DALTON
FULL PAPER

Stereochemical nonrigidity of $[Rh_6(CO)_{15}L]$ clusters in solution †

Elena V. Grachova,[a] Brian T. Heaton,*[b] Jonathan A. Iggo,*[b] Ivan S. Podkorytov,[c] Daniel J. Smawfield,[b] Sergey P. Tunik *[a] and Robin Whyman[b]

[a] *St. Petersburg University, Department of Chemistry, Universitetskii pr., 2, St. Petersburg, 198904, Russia*
[b] *Department of Chemistry, University of Liverpool, P.O. Box 147, Liverpool, UK L69 7ZD*
[c] *S.V. Lebedev Central Synthetic Rubber Research Institute, Gapsalskaya 1, St. Petersburg, 198035, Russia*

Received 1st March 2001, Accepted 3rd October 2001
First published as an Advance Article on the web 1st November 2001

A series of substituted hexarhodium carbonyl clusters $[Rh_6(CO)_{15}L]$ (L = PR_3 (R = alkyl, aryl), $P(OPh)_3$, NCMe, I^-) has been studied by variable temperature and two-dimensional, X-{^{103}Rh}, (X = ^{13}C, ^{31}P) HMQC and ^{13}C EXSY NMR spectroscopy in solution. At low temperatures, the spectra are consistent with retention of the solid state structure. Different localised exchanges of **t**erminal (CO_t) and **f**ace-**b**ridging (CO_{fb}) CO's are found to occur over different atoms of the Rh_6-octahedron at higher temperatures and the different pathways of the exchanges are discussed. When L = PR_3 (R = alkyl, aryl), the lowest energy scrambling surprisingly involves exchange of CO_t and CO_{fb}, associated with the **s**ubstituted rhodium (S-type), with concomitant exchange of L between the two terminal sites on the substituted rhodium, followed by other localised stereospecific exchanges involving CO's associated with **u**nsubstituted rhodium atoms (U-type). For the other substituted clusters (L = $P(OPh)_3$, NCMe, I^-), only U-type exchanges are observed. The kinetics of these exchanges are reported at different temperatures and for the S-type exchange mechanism, the rate is found to vary with the nature of PR_3.

Introduction

The carbonyl ligands in transition metal carbonyl clusters undergo a variety of fluxional processes in solution, which traditionally have been established by variable temperature NMR measurements. For clusters containing a metal with I = 1/2, *e.g.* ^{103}Rh, it has been possible to establish unambiguously both the individual ligand movements and the pathways involved.[1] However, for complexes which do not contain a metal with I = 1/2, the exact rearrangement mechanism often remains controversial, even for trinuclear clusters.[2,3] For higher nuclearity systems, where several independent or interdependent fluxional processes can occur with similar activation energies, it can be difficult to determine unambiguously the ligand migrations involved in each process. 2D EXSY NMR spectroscopy, in principle, allows easy access to the microscopic detail (*i.e.* the individual ligand movements) of the fluxional process provided a firm assignment of the ^{13}CO NMR resonances is available.[4–10] We have recently reported the use of 2D inverse detected HMQC ^{13}C-{^{103}Rh} and ^{31}P-{^{103}Rh} NMR spectroscopy on several substituted derivatives of $[Rh_6(CO)_{16}]$ and other rhodium clusters to assign unambiguously the ^{13}CO NMR spectra of these clusters and to indirectly detect and assign ^{103}Rh resonances.[11–13] In the present paper, we report systematic NMR studies on mono-substituted derivatives of $[Rh_6(CO)_{16}]$, which have been structurally characterised. Unambiguous assignments of the ^{13}CO resonances derived from HMQC measurements together with the results of 2D ^{13}C–^{13}C EXSY measurements have been used to elucidate movements of the different CO's around the cluster skeleton. Analysis of the 1D NMR spectra has also allowed determination of the thermodynamic parameters for the observed exchange process.

† Electronic supplementary information (ESI) available; the relationship between the rate of S-type exchange in $[Rh_6(CO)_{15}(PR_3)]$ and the pK_a' values of the phosphine ligand. See http://www.rsc.org/suppdata/dt/b1/b101962g/

Results

Detailed assignment of the ^{13}C, ^{31}P and ^{103}Rh spectra

As previously pointed out,[14–17] both the number and multiplicity of signals in the low temperature ^{13}C spectra of $[Rh_6(CO)_{15}L]$ in solution are entirely consistent with the C_s symmetry of the solid state structure. ^{13}C-{^{103}Rh} decoupling measurements were used to make a complete assignment of these resonances in the spectra of the $P(OPh)_3$, PPh_3 and I^- substituted clusters,[14] but this is now much more efficiently carried out using 2D HMQC X-{^{103}Rh}, (X = ^{13}C, ^{31}P) measurements. A representative example of the use of these HMQC procedures is given below for $[Rh_6(CO)_{15}L]$ (L = $P(4\text{-Cl-}C_6H_4)_3$), (see Fig. 1a), (L = $P(OPh)_3$), (see Fig. 1b) and the numbering scheme for this type of cluster is schematically shown in Fig. 2.

Assignment of the correlations associated with Rh(A) and Rh(D) in these spectra is straightforward because resonances due to Rh(A) and C(4)O appear in the 1D projection as a doublet and doublet of doublets respectively due to coupling with the phosphorus nucleus. The resonance of Rh(D) correlates with only one doublet in the terminal CO region, C(9)O, whereas both Rh(B) and Rh(C) correlate with the resonances of two different terminal CO groups. Unambiguous assignment of the Rh(B) and Rh(C) correlations and the corresponding resonances in the 1D ^{13}C and ^{103}Rh NMR spectra can be made *via* a consideration of the long range couplings to phosphorus. The Rh resonance at −326 ppm correlates with the CO resonance at 182.3 ppm, which is a doublet of doublets in the 1D spectrum due to ^3J(P–C); resonances of this type were previously assigned[14] to C(8)O on the basis of the *trans-trans* disposition of the CO and phosphorus ligands. This configuration is considered the most favourable for maximizing ^3J(P–C) when compared with a *cis-trans* or *cis-cis* arrangement. This assumption allows the rhodium resonances at −417 and −326 ppm to be assigned to Rh(B) and Rh(C), respectively. Consistent with this assignment in the 1D ^{31}P NMR spectrum of $[Rh_6(CO)_{15}$-

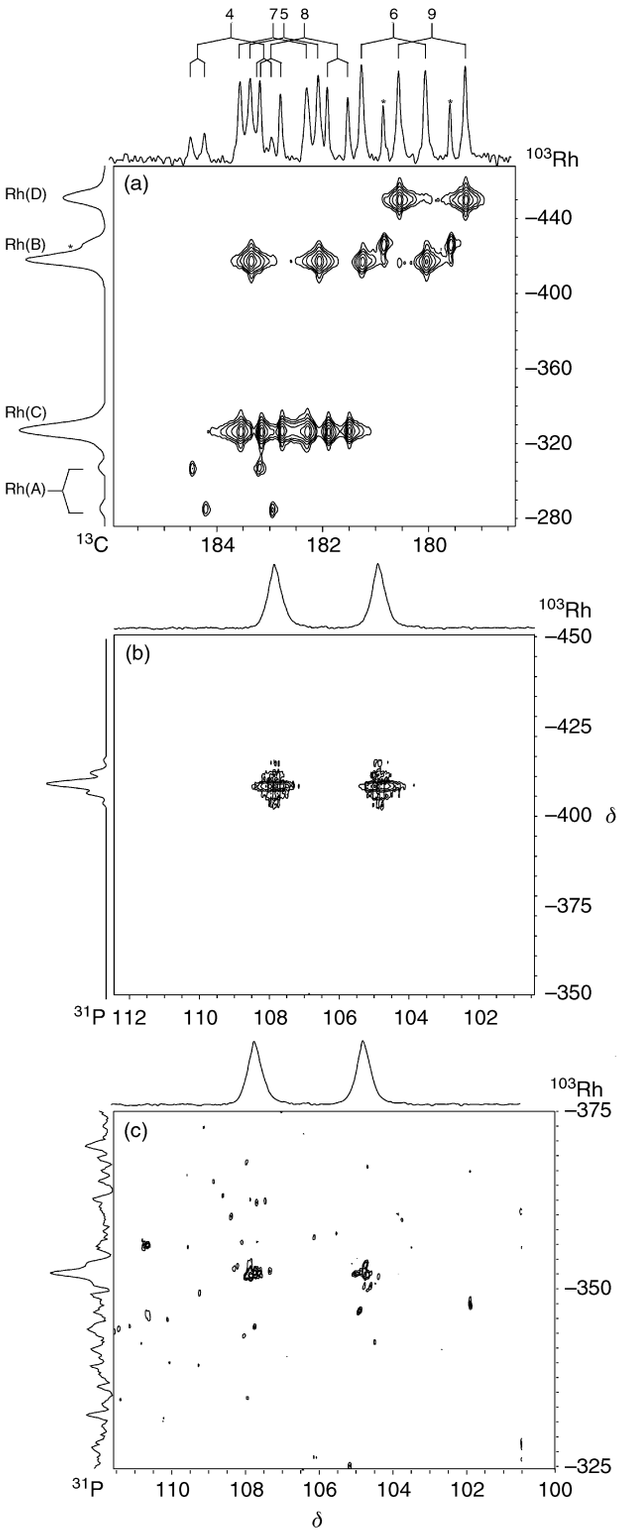

Fig. 1 (a) HMQC ^{13}C-{^{103}Rh} spectrum of [$Rh_6(CO)_{15}$(P(4-Cl-$C_6H_4)_3$)] in $CDCl_3$ at 268 K. (b) HMQC ^{31}P-{^{103}Rh} spectra of [$Rh_6(CO)_{15}(P(OPh)_3)$] in $CDCl_3$ at 298 K, $^1J_{Rh-P}$ = 240 Hz, (c) as (b) $^2J_{Rh-P}$ = 8.6 Hz. see Fig. 2 for labelling scheme.

($P(OPh)_3$)], the phosphorus resonance appears as a well-resolved doublet of triplets corresponding to ^1J(Rh(A)–P) 240 Hz and $^2J(Rh(C)–P)_{trans}$ 8.6 Hz. The ^{31}P-{^{103}Rh} HMQC patterns for [$Rh_6(CO)_{15}(P(OPh)_3)$], tuned to these two values of the coupling constants, (see Fig. 1b) allow the resonances at −410 and −352 ppm to be assigned unambiguously to Rh(A) and Rh(C), respectively and confirm the *trans-trans* nature of three bond ^{31}P–^{13}C couplings that occur in all the ^{13}C spectra of [$Rh_6(CO)_{15}$L] (L = PR_3, R = alkyl or aryl; $P(OPh)_3$). The resonances of C(2)O and C(3)O in the bridging carbonyl region can

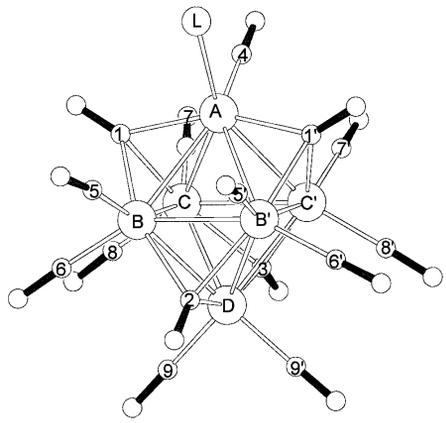

Fig. 2 Schematic representation of the structure of [$Rh_6(CO)_{15}$L] showing the atom-labelling scheme.

then be distinguished by ^{13}C-{^{103}Rh} HMQC measurements. The above analysis clearly demonstrates the ability of the HMQC technique in conjunction with the 1D NMR spectra to assign unambiguously the ^{13}C and ^{103}Rh NMR spectra of these clusters and to establish the solution structure of the P-substituted rhodium carbonyl clusters at a level that is inaccessible by any other spectroscopic method. When L is a non-P-donor, the above procedure for the unambiguous assignment of the ^{13}C and ^{103}Rh resonances cannot be used. For these clusters, we have made the assignment by analogy with the P-donor derivatives, *i.e.* for the two resonances of intensity one due to the face-bridging carbonyls, hereafter CO_{fb}, C(2)O always occurs at lowest field. The ^{13}C, ^{31}P, ^{103}Rh NMR data obtained for the clusters **I** and **III–X** together with their assignments are given in Table 1. HMQC spectra of **II** (L = PEt_3) have not been measured but the VT 1D ^{13}C NMR spectra are very similar to those of **I** and assignments have been made by analogy with **I**.

CO Fluxional processes in [$Rh_6(CO)_{15}$L] from 2D ^{13}C–^{13}C EXSY and ^{13}C VT measurements

^{13}C–^{13}C EXSY spectra of [$Rh_6(CO)_{15}$L] (L = PR_3, R = alkyl or aryl) show that there is a low energy exchange involving a terminal carbonyl ligand, hereafter CO_t, and the two face-bridging CO's, CO_{fb}, associated with the substituted Rh (S-type exchange). This is exemplified by the EXSY spectra of [$Rh_6(CO)_{15}$(P(4-MeO-$C_6H_4)_3$)] (see Fig. 3), which show correlations corresponding to the pairwise exchange of C(1)O with C(4)O, C(2)O with C(3)O, C(5)O with C(7)O, and C(6)O with C(8)O. The rates of each pairwise exchange, evaluated on the basis of the cross peak integrals, are equal and consistent with an overall concerted mechanism, *vide infra*. Variable temperature measurements on the other clusters in this group reveal this to be a general exchange pathway for the mono-phosphine substituted derivatives of [$Rh_6(CO)_{16}$] as exemplified in Fig. 4 for L = P(4-Cl-$C_6H_4)_3$. The exchange rates for this process, k_s, and the activation parameters calculated from the Eyring equation (see Experimental), together with the phosphine basicities are given in Table 2. Although there is a significant variation in pK_a, for the substituted aryl phosphines, there is not much change in $\ln k_s$; the most significant result is found with the more basic trialkylphosphine substituted clusters, which exhibit a much slower rate of C(1)O/C(4)O exchange than is observed with the arylphosphine substituted analogues.

[$Rh_6(CO)_{15}$L] (L = PR_3, R = alkyl or aryl) also exhibits exchange of CO_{fb} with CO_t on the unsubstituted Rh's (U-type exchange). The U-type exchanges are slow in comparison with the S-type exchange referred to above. As a rule, the corresponding cross peaks are visible in the 2D EXSY spectra with rather long mixing times, good S : N ratio and at low contour levels on the 2D map. Thus Fig. 5, L = P(4-MeO-$C_6H_4)_3$, shows

Table 1 NMR spectroscopic data for $[Rh_6(CO)_{16}]$ substituted derivatives (for numbering scheme, see Fig. 2)

	$[Rh_6(CO)_{15}(PBu^n_3)]$ **I**			$[Rh_6(CO)_{15}(P(4\text{-}MeO\text{-}C_6H_4)_3)]$ **III**			$[Rh_6(CO)_{15}(PPh_3)]$ **IV**			$[Rh_6(CO)_{15}(P(4\text{-}F\text{-}C_6H_4)_3)]$ **V**			$[Rh_6(CO)_{15}(P(4\text{-}Cl\text{-}C_6H_4)_3)]$ **VI**			$[Rh_6(CO)_{15}(P(4\text{-}CF_3\text{-}C_6H_4)_3)]$ **VII**			$[Rh_6(CO)_{15}(P(OPh)_3)]$ **VIII**			$[Rh_6(CO)_{15}I]^-$ **IX**[g]		$[Rh_6(CO)_{15}(NCMe)]$ **X**	
	$CDCl_3$, 253 K			$CDCl_3$, 223 K			$CDCl_3$, 250 K			$CDCl_3$, 213 K			$CDCl_3$, 250 K			$CDCl_3$, 213 K			$CDCl_3$, 297 K			$CD_3C(O)CD_3$, 203 K[h]		PhCD$_3$/ CDCl$_3$/ CH$_3$CN = 6/4/1, 297 K	
Assignment	δ (X)	$^1J_{Rh-X}$/ Hz	Other SSCC	δ (X)	$^1J_{Rh-X}$/ Hz	Other SSCC	δ (X)	$^1J_{Rh-X}$/ Hz	Other SSCC	δ (X)	$^1J_{Rh-X}$/ Hz	Other SSCC	δ (X)	$^1J_{Rh-X}$/ Hz	Other SSCC	δ (X)	$^1J_{Rh-X}$/ Hz	Other SSCC	δ (X)	$^1J_{Rh-X}$/ Hz	Other SSCC	δ (X)	$^1J_{Rh-X}$/ Hz	δ (X)	$^1J_{Rh-X}$/ Hz
C(1)O	239.6	19, 26, 33		239.4	16, 31		239.6	19, 19, 20		239.4	19, 28, 32		239.1	20, 29		238.5	21, 27		236.8	21, 28, 31		243.5[h]	36, 24, 17	244.2	30, 34
C(2)O	234.9	29		236.7	28		236.7	27.4		235.8	28		235.5	32		234.7	28		235.0	26.6		238.6[h]	28	233.7[j]	27.7
C(3)O	230.9	28		231.6	29		232.1	28.1		231.4	28		231.5	29		231.0	27		231.6	27.5		231.8[h]	28	230.6[j]	25.9
C(4)O	184.3	70	10.2[b]	184.6	70	13.2[a]	183.3	69.5	13.3[b]	184.2	70	13.6[a]	183.8	70	13.8[b]	183.5	70	14.5[b]	180.9	68.5	10.3[b]	185.3[h]	68	179.8	69.2
C(5)O	184.3	70		182.7	71		182.0	70.2		182.9	70		182.7	70		182.6	70		181.9	70.0		181.9[h]	72	182.8[k]	70.0
C(6)O	180.6	66		181.2	66		180.1	65.8		181.0	66		180.5	66		180.1	66		180.6	66.4		181.2[h]	67	181.3[k]	68.4
C(7)O	183.1	69		184.1	70		182.7	69.7		183.5	69		182.9	69		182.4	69		182.0	69.5		183.0[h]	70	181.2[k]	67.9
C(8)O	182.8	70	18.3[c]	183.4	69	20.3[c]	182.1	69.7	20.7[c]	182.9	70	20.9[c]	182.3	68	22.5[c]	181.8	69	21.8[c]	181.8	68.7	36.3[c]	182.7[h]	69	179.7[k]	68.8
C(9)O	179.9	69		180.4	69		179.4	68.7		180.1	69		179.7	69		179.3	69		180.3	68.3		181.8[h]	69	178.6	69.5
P	16.7	127		23.9	133		25.4	134.6		24.1	138		24.4	139		25.4	139		106.3	240.0	8.6[f]				
Rh(A)[a]	−352			−266			−303[d]			−297			−295			−329[e]			−410			−104[i]		470	
Rh(B)[a]	−427			−416			−445[d]			−426			−417						−405			−405[i]		−400	
Rh(C)[a]	−334			−324			−347[d]			−333			−326						−352			−417[i]		−400	
Rh(D)[a]	−448			−462			−484[d]			−461			−450						−430			−498[i]		−460	

[a] The ^{103}Rh NMR data are from HMQC measurements and are reported at the temperature of measurement. With increasing temperature, there is a shift in $\delta(^{103}Rh)$ of +0.5 ppm K^{-1}. [b] ^2J(P–CO). [c] ^3J(P–CO). [d] ^{103}Rh NMR data obtained in $CDCl_3$ at 213 K from the ^{13}C-{^{103}Rh} NMR measurements. [e] This value was obtained from ^{31}P-{^{103}Rh} HMQC spectra at 290 K. Due to the low solubility of the sample the ^{13}C-{^{103}Rh} HMQC correlations have not been measured. The assignment of the ^{13}C resonances is based on the similarity of the 1D ^{13}C NMR spectra and the observed cluster dynamics with the other phosphine derivatives. [f] ^2J(Rh–P). [g] Data from ref. 16. [h] Recorded in $CD_3C(O)CD_3$ solution, 203 K, not in CD_3CN as stated in ref. 16. [i] Direct ^{103}Rh NMR measurements in $CD_3C(O)CD_3$ at 193 K. [j] Assignments can be interchanged; all resonances of relative intensity 1. [k] Assignments can be interchanged; all resonances of relative intensity 2.

Table 2 Heteroligand basicities, rates and activation parameters for S-type exchange in $[Rh_6(CO)_{15}(PR_3)]$

R	Bu^n, **I**		Et, **II**		4MeO-C_6H_4, **III**		Ph, **IV**		4-F-C_6H_4, **V**		4-Cl-C_6H_4, **VI**		4-CF_3-C_6H_4, **VII**	
Rate constants, k_S, for S-type exchange at different temperatures	T/K	k_S/s^{-1}	T/K	k_S/s^{-1}	T/K	k_S/s^{-1}	T/K	k_S/s^{-1}	T/K	k_S/s^{-1}	T/K	k_S/s^{-1}	T/K	k_S/s^{-1}
	298	2.2	295	2.2	264	4.2	250	3.0	252	2.0	252	2.7	246	1.7
	306	4.4	301	3.8	270	7.7	255	4.0	258	4.6	258	4.7	252	3.1
	312	9.0	306	6.6	274	14	260	6.6	264	8.3	264	10	258	4.9
	317	14	312	12	280	27	267	11	270	16	270	17	264	10
	322	28	317	22			272	19	274	33	274	46	270	30
			322	33			276	27						
$\Delta H^{\#}$/kJ mol^{-1}	82 ± 5		83 ± 3		70 ± 4		47 ± 2		67 ± 4		68 ± 7		61 ±7	
$\Delta S^{\#}$/J mol^{-1} K^{-1}	40 ± 20		30 ± 10		30 ± 20		−49 ± 9		30 ± 20		30 ± 30		10 ± 30	
$\Delta G^{\#}$(273 K)/kJ mol^{-1}	72.1 ± 0.6		71.0 ± 0.6		61.0 ± 0.1		59.9 ± 0.1		59.3 ± 0.2		58.9 ± 0.4		58.9 ± 0.5	
pK_a [a]	8.67		7.96		5.13		3.28		1.63		0.87		−1.39	

[a] The data were taken from ref. 38.

Fig. 3 ^{13}C EXSY spectrum showing S-type exchange correlations in $[Rh_6(CO)_{15}(P(4\text{-}MeOC_6H_4)_3)]$, **III**, in $CDCl_3$ at 274 K; τ_{mix} = 0.02 s. See Fig. 2 for labelling scheme.

that C(1)O also correlates with C(5)O and C(6)O and C(9)O with C(3)O.

For the non-phosphine substituted clusters $[Rh_6(CO)_{15}L]$ (L = $P(OPh)_3$, NCMe, I^-), there is no evidence for the S-type of CO_t/CO_{fb} exchange, even at high temperature. However, there is evidence for U-type CO_t/CO_{fb} exchanges, but these only occur at temperatures which are significantly higher than those

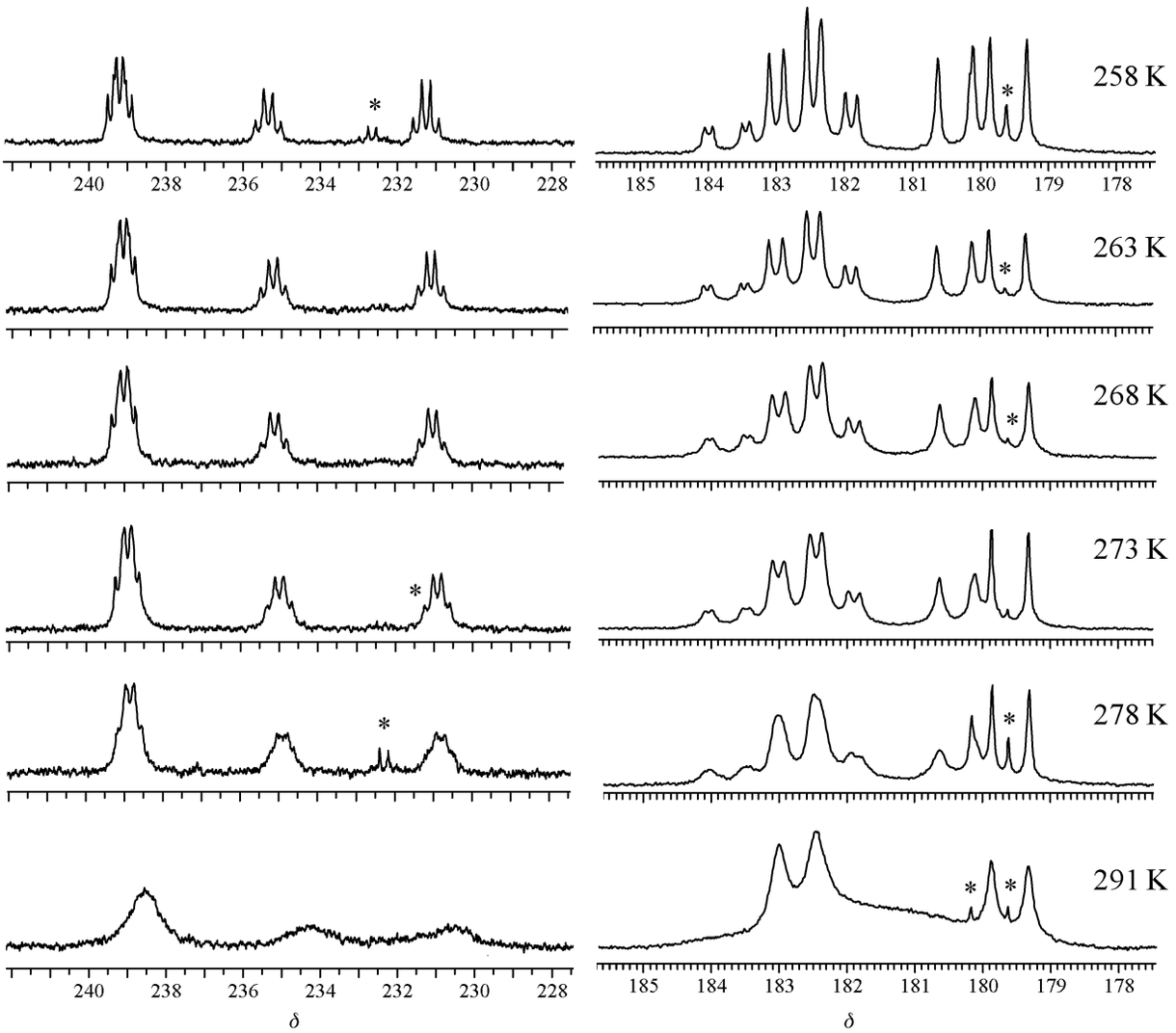

Fig. 4 Variable temperature ^{13}C NMR spectra of the carbonyl resonances for $[Rh_6(CO)_{15}(P(4\text{-}Cl\text{-}C_6H_4)_3)]$ in $CDCl_3$. The resonances marked with an asterisk correspond to $[Rh_6(CO)_{16}]$, present as an impurity.

required for S-type exchange in the phosphine substituted clusters. When L = $P(OPh)_3$, NCMe, I^-, the EXSY spectra of all these substituted clusters exhibit a correlation between C(3)O and C(7)O, C(8)O and C(9)O (see Fig. 5b) and, additionally, for L = $P(OPh)_3$, a correlation linking C(1)O with C(5)O and C(6)O is observed; this last exchange is an order of magnitude slower than the exchanges observed for C(3)O. All these correlations, together with the rates of S- and U-type exchanges at different temperatures are summarised in Table 3.

Discussion

S-Type CO scrambling in $[Rh_6(CO)_{15}L]$ (L = PR_3, R = alkyl or aryl)

The S-type of exchange involves exchange only of C(1)O with C(4)O, together with an oscillation of L between the two terminal sites on Rh(A), (see Scheme 1). This localised movement results in the symmetry related transformations of C(2)O and C(3)O, C(5)O and C(7)O, C(6)O and C(8)O, in accord with the observed EXSY correlations (see Fig. 3 and Table 3).

The exact mechanism of this S-type exchange (see Scheme 2) could involve either transformation of the **f**ace-bridging C(1)O ligand into an **e**dge-bridging and then into a **t**erminal (**FET**) or the direct shift of C(1)O into a terminal site on Rh(A) followed by a **t**urn**s**tile **r**otation (**TSR**). It is difficult to distinguish between these two mechanisms, although the **FET** movement seems likely for the following reasons:

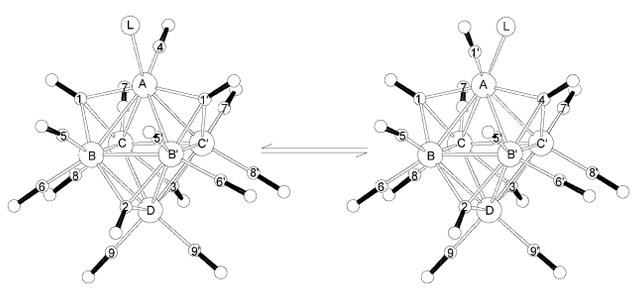

Scheme 1 S-Type exchange found in the clusters **I–VII**.

(a) **FET** involves the concerted breaking/formation of Rh–CO bonds, whereas the **TSR** mechanism requires simultaneous breaking of two Rh–CO_{fb} bonds followed by rotation,

(b) the **TSR** mechanism would be expected to be more difficult for a $M(CO)_2L$-group than for a $M(CO)_3$-group,[18,19]

(c) as shown by one of us previously,[20] the C(1)O face-bridging ligand is always asymmetrically bonded to the Rh(A)Rh(B)Rh(C)-face for *all* mono-substituted derivatives of $[Rh_6(CO)_{16}]$, which have been characterised by X-ray crystallography: C(1)O lies closer to the Rh(A)–Rh(B) edge and *d*(Rh(A)–C(1)) is always the shortest (see Table 4) as required for the **FET** pathway. Related to these solid state observations, pronounced variations are observed for ^1J(Rh–C(1)O) in solution. We have previously shown that ^1J(Rh–CO) correlates strongly with the Rh–C bond length for CO_{fb}.[16,21,22] Although it has not been possible to assign unambiguously all the values of

Table 3 The data for U-type CO_{fb}/CO_t exchanges in $[Rh_6(CO)_{15}L]$ (for numbering scheme see Fig. 2)

			U-type CO_{fb}/CO_t exchange						
				C(1)O		C(2)O		C(3)O	
L	T/K	k_S/s^{-1}	τ_{mix}/s		k/s^{-1}		k/s^{-1}		k/s^{-1}
PBu^n_3, **I**	298	2.2	0.1	1 ↔ (5,6)	0.9	2 ↔ 9	0.7	3 ↔ 9	1.6
$P(4\text{-MeO-}C_6H_4)_3$, **III**	274	14.0	0.02	1 ↔ (5,6)	3	2 ↔ 9 vw	0.2	3 ↔ 9	1.0
PPh_3, **IV**	270	15.6	0.04	1 ↔ (5,6)	*ca.* 5				
$P(4\text{-F-}C_6H_4)_3$, **V**	264	8.3	0.017	1 ↔ (5,6)	0.6	2 ↔ 9	0.4	3 ↔ 9	0.4
$P(OPh)_3$, **VIII**	322	—	0.5	1 ↔ (5,6)	0.07	2 ↔ (5,6)	1.0	3 ↔ 9	0.9
						2 ↔ 9	0.3	3 ↔ (7,8)	2.0
I^-, **IX**	301	—	0.1					3 ↔ (7,8) [a]	8.0
								3 ↔ 9 [b]	4.0
NCMe, **X**	312	—	0.1					3 ↔ (7,8) [a]	3.0
								3 ↔ 9 [b]	1.0

[a] Assignment could be reversed to 2 ↔ (5,6). [b] Assignment could be reversed to 2 ↔ 9.

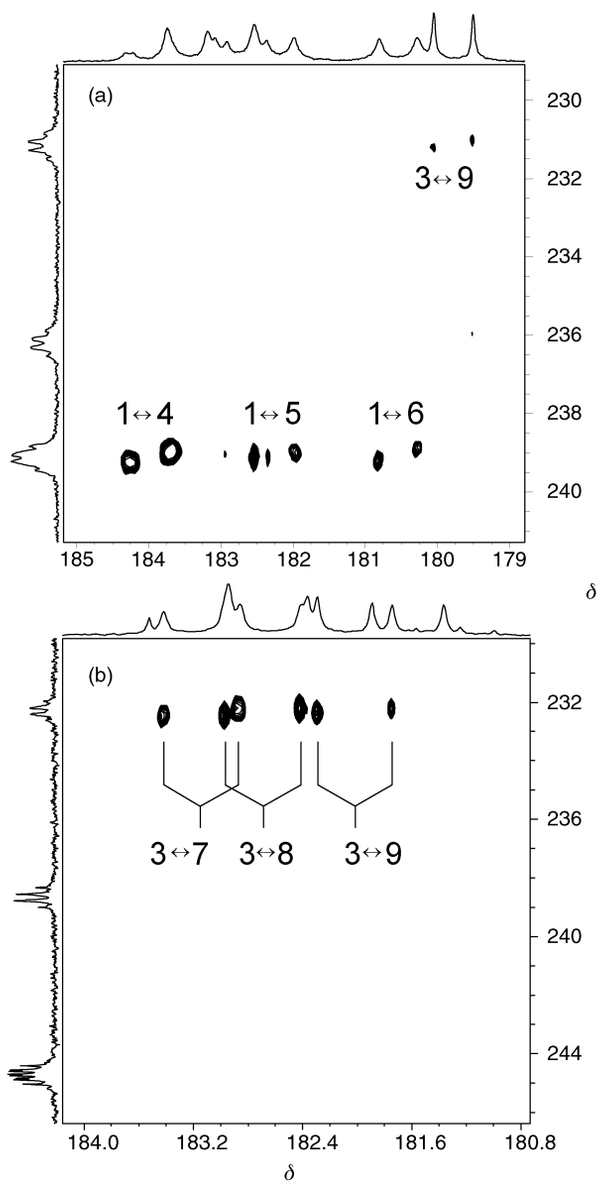

Fig. 5 (a) ^{13}C EXsY spectrum showing U-type exchange correlations in $[Rh_6(CO)_{15}(P(4\text{-MeOC}_6H_4)_3)]$, in $CDCl_3$ at 274 K; τ_{mix} = 0.02 s. See Fig. 2 for labelling scheme. (b) ^{13}C EXSY spectrum showing the terminal/bridging carbonyl correlations in $[Rh_6(CO)_{15}I]^-$, in $CDCl_3$ at 301 K; τ_{mix} = 0.1 s. See Fig. 2 for labelling scheme.

^1J(Rh–C(1)O) to the different rhodium atoms directly from HMQC measurements, we can make reasonable assignments based on previous work and Fig. 6 plots the variation in

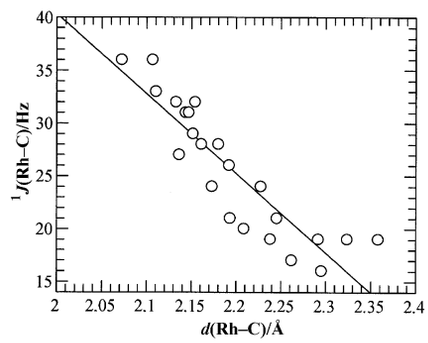

Fig. 6 Variation in d(Rh–C(1)O) and ^1J(Rh–C(1)O) for the phosphorus donor **I–VII** and halide **VIII**, **IX** substituted derivatives of $[Rh_6(CO)_{16}]$. Correlation coefficient (R) = −0.894.

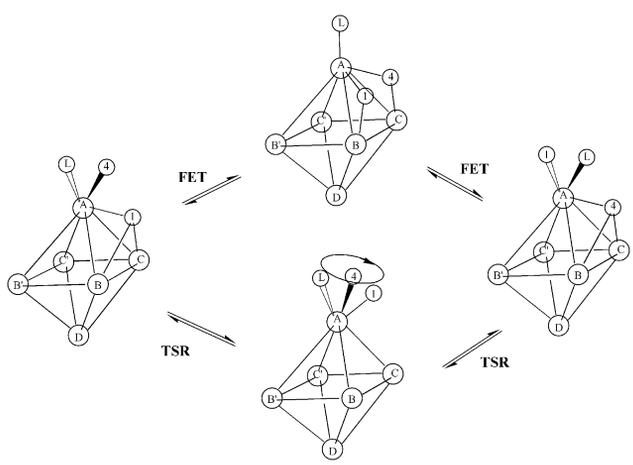

Scheme 2 Possible mechanism of exchange of CO_t/CO_{fb} in $[Rh_6(CO)_{15}L]$: L = PR_3, (R = alky, aryl) for S-type exchange; L = CO for U-type exchange.

^1J(Rh–CO) for CO_{fb} with d(Rh–C), suggesting that the solid state distortions observed in $[Rh_6(CO)_{15}L]$ are also retained in solution.

(d) analysis of the non-bonding contacts in $[Rh_6(CO)_{15}L]$ shows that there is a displacement of C(4)O towards Rh(C); in statistical terms, this is significantly greater than the distortion of *all* other terminal CO's towards analogous non-bonded Rh's when L = PR_3 (R = alkyl, aryl), $P(OPh)_3$ but this displacement does *not* occur when L = NCMe, I^-,

(e) there is a wide variation in the unit cell adopted by the substituted clusters listed in Table 4, and it therefore seems unlikely that the systematic distortions described above are due to either intra- or inter-cluster packing effects.

Since all the presently studied $[Rh_6(CO)_{15}L]$ clusters exhibit asymmetric bonding of C(1)O to the Rh(A)Rh(B)Rh(C)-

Table 4 Structural data related to C(1)O and C(4)O, and the values of ^1J(Rh-C) for mono-substituted clusters, $[Rh_6(CO)_{15}L]$

L	d(Rh(X)–C(1))/Å [a]			^1J(Rh(X)–C(1)O)/Hz			*cis*-Rh–(Rh)–C non-bonding contact/Å		
	X = A	X = B	X = C	X = A	X = B	X = C	d(Rh(C)–C(4)) averaged for Rh(C) and Rh(C′)	Averaged for all other terminal CO's, excluding C(4)O, d_{av}	$d - d_{av}$
$P(Bu^n)_3$, **I** [20]	2.110	2.192	2.238	33	26	19	3.451	3.540 ± 0.009	−0.089
$P(4\text{-MeO-}C_6H_4)_3$, **III** [20]	2.144	2.194	2.295	31	16	16	3.370	3.542 ± 0.008	−0.172
PPh_3, **IV** [17]	2.154	2.180	2.324	32	28	19	3.361	3.564 ± 0.008	−0.203
$P(4\text{-F-}C_6H_4)_3$ **V** [20]	2.133	2.162	2.358	32	28	19	3.398	3.569 ± 0.018	−0.171
$P(4\text{-Cl-}C_6H_4)_3$, **VI** [20]	2.152	2.209	2.293	29	20	20	3.427	3.578 ± 0.007	−0.151
$P(4\text{-CF}_3\text{-}C_6H_4)_3$, **VII** [20]	2.137	2.193	2.256	27	21	21	3.396	3.550 ± 0.006	−0.154
$P(OPh)_3$, **VIII** [20]	2.147	2.161	2.246	31	28	21	3.434	3.520 ± 0.006	−0.086
I^-, **IX** [31]	2.072	2.173	2.262	36	24	17	3.562	3.493 ± 0.002	0.069
NCMe, **X** [20]	2.170	2.205	2.205	34	30	30	3.525	3.521 ± 0.001	0.004
Cl^- [32]	2.107	2.228	2.292	36	24	19	3.504	3.542 ± 0.003	−0.038

[a] Values given in the Table have been averaged for C(1)O and C(1′)O, which are essentially equivalent.

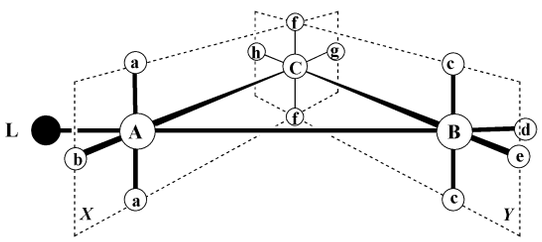

Fig. 7 CO-Exchange observed in $[Os_3(CO)_{11}L]$ (L = $P(OMe)_3$, PEt_3), together with the CO labelling scheme.

triangle, the displacement of C(4)O to Rh(C) is perhaps a better indicator for S-type exchange, involving the **FET** mechanism. However, although all the phosphine substituted derivatives exhibit this displacement and undergo S-type exchange, the $P(OPh)_3$ derivative is an exception since it also exhibits the same displacement but does *not* undergo S-exchange! As a result, there must be additional factors, which (very probably, in combination with the above mentioned parameters) are responsible for this localised S-type exchange.

There are few known examples of CO fluxional processes which involve a CO_{fb} present in the ground state.[23,24] As a result, comparison with structural distortions in other clusters, which undergo CO-exchange *via* different mechanisms, is not useful. However, it is generally observed that the rate of CO-exchange by any mechanism is enhanced by phosphine substitution. Thus, VT ^{13}C NMR measurements (25 MHz) [25] have shown that $[Rh_6(CO)_{16}]$ is static at +70 °C, whereas S-type exchange in $[Rh_6(CO)_{15}L]$ (L = PR_3, R = alkyl, aryl) starts to occur at temperatures ≤0 °C. What is unusual about the S-type of exchange in these phosphine substituted Rh_6-carbonyl clusters is the concomitant movement of L in the lowest energy exchange process since in other simple phosphine substituted metal carbonyl clusters (*i.e.* those that do not contain other heteroligands), the phosphines usually remain static and usually block or substantially retard CO-migrations. Although there is a small number of examples of phosphine substituted, carbonyl clusters that contain additional heteroligands in which the lowest energy carbonyl migration pathway involves both the additional heteroligand and the phosphine,[4] it is most useful to compare structures which do not contain the complication of additional heteroligands and which retain the same basic CO distribution on the metal skeleton upon substitution, *e.g.* $[Os_3(CO)_{12-x}L_x]$ (x = 0, 1; L = P-donor ligand).[26–29] In this case, substitution by a P-donor ligand results in a significant increase in carbonyl mobility about the substituted and adjacent unsubstituted metal and the lowest energy migrational process in $[Os_3(CO)_{11}L]$ involves terminal/edge carbonyl exchange but does *not* involve movement of the P-donor (see Fig. 7). Initially, only CO's a,b,f, and g are involved, *via* rotation in plane *X*; CO(h) and L are both static.[28,29] Furthermore, there is clear evidence that L blocks analogous CO migrations when L is in the rotation plane. Thus, the CO's on Os(B) (c, and e) undergo preferential exchange with f and h in the analogous plane, *Y*.

In an alternative approach, the **L**igand and **P**olyhedral **M**odel (**LPM**) has been used to explain the behaviour of $[Os_3(CO)_{11}L]$.[30] However, we believe that the **LPM** cannot be used to account for, in particular, the S-type exchange in these substituted Rh_6-clusters; therefore we prefer to consider localised exchanges of the ligands on the metal skeleton rather than movement of the metal skeleton within the ligand framework.

U-Type CO scrambling in $[Rh_6(CO)_{15}L]$ (L = PR_3 (R = alkyl, aryl), $P(OPh)_3$, NCMe, I^-)

All of the clusters studied exhibit U-type exchanges involving localised exchange of CO_{fb} with CO_t about the unsubstituted Rh's at observed rates which are usually significantly lower than those for the S-type exchange (see Table 3); moreover, the CO's involved in this U-type exchange depend very much upon the nature of L, *vide infra*. Localised CO_{fb}/CO_t exchanges can occur about any one of the three unsubstituted rhodiums, Rh(B), Rh(C), Rh(D). Thus, all the clusters exhibit U-type exchange of C(3)O with C(9)O. Phosphine substituted clusters also exhibit exchange of C(1)O with C(5)O and C(6)O and of C(2)O with C(9)O. This last exchange also occurs when L = $P(OPh)_3$ as does exchange of C(2)O with C(5)O and C(6)O. For both the non-phosphine clusters, C(3)O also exchanges with C(7)O and C(8)O. Thus, different ligands induce different U-type exchanges involving different CO's on different parts of the Rh_6-skeleton. These data are summarised in Table 3. The mechanism of the U-type of CO exchange is presumably related to the S-type and could involve either the **FET**- or **TSR**-route, (see Scheme 2).

An unexpected feature of these closely related clusters, is that there should be such a large difference both in the rates of CO migration (S-*versus* U-type exchanges) and in the sites which are involved in these localised exchanges. It is worthwhile noting that, although there is a large variation in the rate of CO_{fb}/CO_t-exchange, k_S, for phosphine substituted clusters, there is no clear relationship between k_S and $pK_{a'}$ within this series (see ESI, Fig. S1). All the clusters containing substituted aryl phosphines, which have a $pK_{a'}$ from −1.39 to 5.13, have similar values of k_S; in contrast k_S is very much lower for clusters containing the more basic trialkyl phosphines, PR_3, (R = Et, Bu^n).

In view of the lack of any clear correlation between the rate of S-type exchange with any one parameter, *e.g.* structural distortions or $pK_{a'}$ values, we feel that the dynamic ligand effects cannot be quantified on the basis of just one selected parameter/property. As a result, steric *and* electronic effects induced by L must be important in determining *both* the mechanism and the particular site(s) of CO ligand exchange together

with the rates of these exchanges. Unfortunately, the ligand effects in clusters are still poorly understood even for rationalising ground state properties. As a result, despite careful structural and NMR studies on a wide range of substituted Rh_6-clusters, both the sites and rates of the observed CO-exchanges in $[Rh_6(CO)_{15}L]$ are difficult to rationalise. Nevertheless, this work has revealed a *new* and unexpected, energetically favourable exchange process, S-type, in phosphine-substituted Rh_6-clusters.

Conclusions

This systematic study of closely related monosubstituted derivatives of $[Rh_6(CO)_{16}]$ has shown that:-

- the CO's involved in intramolecular exchange are strongly dependent on the nature of L,
- the S-type of CO_t/CO_{fb} exchange involving the substituted Rh atom, with concomitant movement of L, only occurs for phosphine substituted clusters; of the phosphines studied, triarylphosphines have the most pronounced activating effect,
- localised U-type exchanges of CO_t/CO_{fb} occur on the other unsubstituted Rh's and the ligands and sites involved are very dependent on L,
- S-type exchanges are faster than U-exchanges; structural distortions suggest the **FET** mechanism for S-exchange,
- the S-type of exchange must necessarily involve movement of L, which is unusual,
- both S- and U-type exchanges involve CO_{fb}, which is also unusual,
- the driving forces for these processes are unclear and probably depend on both structural and electronic effects induced by L.

Experimental

Reagents and solvents

The substituted $[Rh_6(CO)_{16}]$ derivatives were synthesized according to previously published procedures: $[Rh_6(CO)_{15}L]$, L = PBu^n_3 **I**,[20] PEt_3 **II**,[20] P(4-MeO-C_6H_4)$_3$ **III**,[20] PPh_3 **IV**,[33] P(4-F-C_6H_4)$_3$ **V**,[20] P(4-Cl-C_6H_4)$_3$ **VI**,[20] P(4-CF_3-C_6H_4)$_3$ **VII**,[20] $P(OPh)_3$ **VIII**,[20] I^- **IX**,[34] NCMe **X**.[35] All solvents were dried over appropriate reagents and distilled prior to use. Reactions were carried out under dry argon. Products were purified in air by column chromatography on silica (5/40 mesh).

NMR measurements

1D 125 MHz ^{13}C-{^1H} variable temperature and 2D phase sensitive ^{13}C–^{13}C-{^1H} EXSY spectra were measured on a Bruker AM-500 NMR spectrometer equipped with a 10 mm broadband probehead. To decrease the longitudinal relaxation time, a relaxation agent was usually added (*ca.* 30 mg of $[Cr(acac)_3]$ to *ca.* 150 mg of 20% ^{13}CO enriched cluster in 3.5 mL of $CDCl_3$). A standard Bruker microprogram, noesyph.au, was used to obtain the 2D EXSY spectra. Typical conditions for the 2D spectra are: relaxation delay 2 s; mixing time in the range 20 to 200 ms, and the actual values are reported in the corresponding Figures and Tables; 64 scans; 4096 and 256 data points in F2 and F1 directions, respectively; π/2 shifted sine bell squared apodization in both dimensions; digital resolution of 5 and 20 Hz/point in F2 and F1 directions, respectively.

Determination of the rate of the S-type exchange process from ^{13}C VT spectra

The temperature dependence of the rate constant k_S for the S-type scrambling in which there is exchange of C(1)O and C(1′)O with C(4)O:

$$2C(1)O \underset{2k_S}{\overset{k_S}{\rightleftharpoons}} C(4)O$$

for the clusters **III–VII** was calculated from exchange broadening b_6 of the C(6)O doublet in the 125 MHz ^{13}C-{^1H} variable temperature spectra. The broadening, b_6, arises from the symmetry related transformation:

$$C(6)O \underset{2k_S}{\overset{2k_S}{\rightleftharpoons}} C(8)O$$

which is generated by S-type scrambling. In the limit of slow exchange [36] and neglecting U-type scrambling:

$$k_S = \pi\, b_6/2$$

The carbonyl C(9)O is not involved in dynamic exchange nor symmetry related transformations, which allows the line width, Δf_9, to be a reasonable estimation for the line width Δf_6 of the resonance due to C(6)O in the absence of exchange; this allows calculation of the exchange broadening as $b_6 = \Delta f_6 - \Delta f_9$. Both the C(6)O and C(9)O doublets are well separated from the other resonances and this allows the rates to be calculated more accurately. We used two distinct algorithms to estimate Δf_6 and Δf_9. The first uses the standard procedure in the Bruker 1D WinNMR program. It treats the two doublets as four independent Lorentzian lines with no constraints on their intensities and line widths. The second algorithm (written in Mathcad) considers the two doublets as four Lorentzian lines of equal intensity; one of the pairs of lines is described by Δf_6 and the other pair by Δf_9. Because of the non-Lorentzian line shape, the presence of spinning side bands and superimposed additional peaks due to impurities, estimations of the broadening b_6 obtained by these two methods differ by a factor of up to *ca.* 1.5. Comparison of b_6, obtained on different samples of the same cluster at different times, leads to approximately the same uncertainty factor, 1.5. This gives an error of 0.4 in $\ln(k_S)$.

For cluster **I**, the procedure described above cannot be used because the rate of U-type exchange is significant and this involves both C(6)O and C(9)O. Namely, C(6)O is broadened not only by the S-type process but also by U-type exchange:

$$C(1)O \underset{k_{651}}{\overset{2k_{156}}{\rightleftharpoons}} \{C(5)O + C(6)O\}$$

C(9) is broadened by two U-type processes:

$$C(2)O \underset{k_{92}}{\overset{2k_{29}}{\rightleftharpoons}} 2C(9)O$$

and

$$C(3)O \underset{k_{93}}{\overset{2k_{39}}{\rightleftharpoons}} 2C(9)O$$

The rate constants for these S- and U-type exchanges, 298 K, were obtained from the 2D ^{13}C EXSY spectrum using the literature procedure;[37] $k_S = 2.2 \pm 0.2$, $k_{39} = 1.6 \pm 0.2$, $k_{156} = 0.9 \pm 0.3$, and $k_{29} = 0.7 \pm 0.1$ s^{-1}.

Using these values of k_S and k_{156} and assuming that $\Delta H^{\#}_{156} = \Delta H^{\#}_S$, the rate constant k_S was determined at several temperatures from the line widths of the C(6)O resonance under the slow exchange limit approximation. The estimation $\Delta H^{\#}_{156} = \Delta H^{\#}_S$ can be considered as a reasonable approximation because the activation parameters of the scrambling processes vary over quite a narrow range.

We did not perform a 2D EXSY experiment for cluster **II**, and rates for the U-type exchanges were not measured for this compound. However, the variable temperature spectra of **II** are similar to **I**. Therefore, we assume that U-type exchanges in **II** are similar to those established for **I**. We also assume that the S-type exchange in **II** is responsible for 70% of the broadening of b_6 as found for **I**. At 280 K, the exchange is not observable, and both the resonances due to C(6)O and C(9)O in **II** have

equal line widths (5.8 Hz). This value was used as the unperturbed line width of C(6)O to evaluate b_6 in the variable temperature spectra. This allows calculation of the activation parameters for the S-type scrambling in **II**.

HMQC measurements were carried out as described previously.[11]

Acknowledgements

We thank EPSRC, INTAS/RFBR (to B. T. H., J. A. I., I. S. P., S. P. T., Grant No. 95-IN-RU-242), INTAS (to E. V. G., Grant No. YSF99–4030) for financial support, EPSRC for an earmarked studentship (to D. J. S.), and the Leverhulme Foundation for a Research Fellowship (to B. T. H.).

References

1 B. T. Heaton, J. A. Iggo, I. S. Podkorytov, D. J. Smawfield and S. P. Tunik, *Metal Clusters in Chemistry*, ed. P. Braunstein, L. Oro and P. Raithby, Wiley-VCH, Weinheim, Germany, 1999, 960.
2 B. E. Mann, *J. Chem. Soc., Dalton Trans.*, 1997, 1457 and references therein.
3 B. F. G. Johnson, *J. Chem. Soc., Dalton Trans.*, 1997, 1473.
4 L. J. Farrugia and S. E. Rae, *Organometallics*, 1991, **10**, 3919; L. J. Farrugia and S. E. Rae, *Organometallics*, 1992, **11**, 196.
5 G. Bondietti, G. Laurenczy, R. Ros and R. Roulet, *Helv. Chim. Acta*, 1994, **77**, 1869; A. Strawczynski, C. Hall, G. Bondietti, R. Ros and R. Roulet, *Helv. Chim. Acta*, 1994, **77**, 754; M. J. Davis and R. Roulet, *Inorg. Chim. Acta*, 1992, **197**, 15.
6 P. J. Bailey, L. H. Gade, B. F. G. Johnson and J. Lewis, *Chem. Ber.*, 1992, **125**, 2019.
7 S. Aime, W. Dastru, R. Gobetto and A. J. Arce, *Organometallics*, 1994, **13**, 3737.
8 D. Wang, H. Shen, M. G. Richmond and M. Schwartz, *Organometallics*, 1995, **14**, 3636.
9 M. P. Cifuentes, M. G. Humphrey, B. W. Skelton and A. H. White, *J. Organomet. Chem.*, 1996, **507**, 163.
10 S. M. Waterman and M. G. Humphrey, *Organometallics*, 1999, **18**, 3116.
11 B. T. Heaton, J. A. Iggo, I. S. Podkorytov, D. J. Smawfield, S. P. Tunik and R. Whyman, *J. Chem. Soc., Dalton Trans.*, 1999, 1917.
12 J. S. Z. Sabounchei, B. T. Heaton, J. A. Iggo, C. Jacob and I. S. Podkorytov, *J. Cluster Sci.*, 2001, **12**, 430.
13 J. S. Z. Sabounchei B. T. Heaton J. A. Iggo C. Jacob, unpublished work.
14 S. P. Tunik, I. S. Podkorytov, B. T. Heaton, J. A. Iggo and J. Sampanthar, *J. Organomet. Chem.*, 1998, **550**, 222.
15 B. T. Heaton, L. Strona, S. Martinengo, D. Strumolo, R. J. Goodfellow and I. H. Sadler, *J. Chem. Soc., Dalton Trans.*, 1982, 1499.
16 C. Allevi, S. Bordoni, C. P. Clavering, B. T. Heaton, J. A. Iggo and C. Seregni, *Organometallics*, 1989, **8**, 385.
17 S. P. Tunik, A. V. Vlasov, N. I. Gorshkov, G. L. Starova, A. B. Nikol'skii, M. I. Rybinskaya, A. S. Batzanov and Yu. T. Struchkov, *J. Organomet. Chem.*, 1992, **433**, 189.
18 H. Wadepohl, D. Braga and F. Grepioni, *Organometallics*, 1995, **14**, 24.
19 T. Beringhelli, G. D'Alfonso and A. P. Minoja, *Organometallics*, 1991, **10**, 394.
20 D. H. Farrar, E. V. Grachova, A. Lough, C. Patirana, A. J. Poë and S. P. Tunik, *J. Chem. Soc., Dalton Trans.*, 2001, 2015.
21 L. Garlaschelli, A. Fumagalli, S. Martinengo, B. T. Heaton, D. O. Smith and L. Strona, *J. Chem. Soc., Dalton Trans.*, 1982, 2265.
22 B. T. Heaton, L. Strona, R. Della Pergola, J. L. Vidal and R. Schoening, *J. Chem. Soc., Dalton Trans.*, 1983, 1941.
23 D. Wang, H. Shen, M. G. Richmond and M. Schwartz, *Organometallics*, 1995, **14**, 3636.
24 C. P. Casey, R. A. Widenhoefer, S. L. Hallenbeck, R. K. Hayashi and J. A. Gavney, *Organometallics*, 1994, **13**, 4720.
25 B. T. Heaton, A. D. C. Towl, P. Chini, A. Fumagalli, D. J. A. McCaffrey and S. Martinengo, *J. Chem. Soc., Chem. Commun.*, 1975, 523.
26 S. Aime, O. Gambino, L. Milone, E. Sappa and E. Rosenberg, *Inorg. Chim. Acta*, 1975, **15**, 53.
27 A. A. Koridze, O. A. Kizas, N. M. Astakhova, P. V. Petrovskii and Y. K. Grishin, *J. Chem. Soc., Chem. Commun.*, 1981, 853.
28 B. F. G. Johnson, J. Lewis, B. E. Reichert and K. T. Shorpp, *J. Chem. Soc., Dalton Trans.*, 1976, 1403.
29 R. F. Alex and R. K. Pomeroy, *Organometallics*, 1987, **6**, 2437.
30 B. F. G. Johnson and A. Bott, *J. Chem. Soc., Dalton Trans.*, 1990, 2437.
31 V. G. Albano, P. L. Bellon and M. Sansoni, *J. Chem. Soc. A*, 1971, 678.
32 A. L. Rheingold, C. B. White, P. D. Macklin and G. L. Geoffroy, *Acta Crystallogr., Sect. C*, 1993, **49**, 80.
33 S. P. Tunik, A. V. Vlasov, A. B. Nikol'skii, V. V. Kryvikh and M. I. Rybinskaya, *Metallorg. Khim.*, 1990, **3**, 387 (in Russian).
34 P. Chini, S. Martinengo and G. Giordano, *Gazz. Chim. Ital.*, 1972, **102**, 330.
35 S. P. Tunik, A. V. Vlasov and V. V. Kryvikh, *Inorg. Synth.*, 1996, **31**, 239.
36 R. R. Ernst, G. Bodenhausen, A. Wokaun, *Principles of Nuclear Magnetic Resonance in One and Two Dimensions*, Clarendon Press, Oxford, 1987.
37 E. W. Abel, T. P. J. Coston, K. G. Orrell, V. Šik and D. Stephenson, *J. Magn. Reson.*, 1986, **70**, 34.
38 L. Chen and A. J. Poe, *Coord. Chem. Rev.*, 1995, **143**, 265.